

# Cell Gap-Dependent Transmittance Characteristic in a Fringe Field-Driven Homogeneously Aligned Liquid Crystal Cell with Positive Dielectric Anisotropy

Seung Jai KIM, Hyang Yul KIM, Seung Hee LEE\*, Yong Kyun LEE<sup>1</sup>, Kyu Chang PARK<sup>1</sup> and Jin JANG<sup>1</sup>

School of Advanced Materials Engineering, Chonbuk National University, Chonju-si, Chonbuk 561-756, Korea

<sup>1</sup>Department of Information Display, Kyunghee University, Seoul 130-701, Korea

(Received February 2, 2005; accepted March 21, 2005; published September 8, 2005)

Transmittance characteristic in a homogeneously aligned liquid crystal (LC) cell driven by a fringe-electric field is investigated as a function of cell gap using the LC with positive dielectric anisotropy. In this device, the fringe-electric field drives the LCs to rotate so that the dielectric torque is electrode-positional dependent, which results in electrode-position dependency in the LC's rotating angle. As the cell gap decreases to 2 μm, more LCs are affected by surface anchoring, and the LCs above the center of electrodes, in which the LCs are twisted by elastic force between neighboring molecules, are less twisted compared to the 4 μm cell. Consequently, when the cell gap decreases from 4 to 2 μm, the transmittance also decreases even though the cell retardation value remains the same. [DOI: 10.1143/JJAP.44.6581]

KEYWORDS: fringe-field switching, cell gap, positive dielectric anisotropy

## 1. Introduction

Recently, the image quality of liquid crystal displays (LCDs) was greatly improved with the development of new conceptual LC modes, such as the in-plane switching (IPS) mode<sup>1-3)</sup> and fringe-field switching (FFS) mode.<sup>4-7)</sup> In both modes the LC director rotates almost in plane; however, their electro-optic characteristics differ significantly from one another.

In the FFS mode, the LCs are homogeneously aligned initially, and the fringe-electric field drives the LCs to rotate. Since the driving field is a fringe-electric field that has both horizontal and vertical components, the field-respondent behavior of the LC is strongly dependent on the sign of the dielectric anisotropy of the LC. For instance, the rubbing angle-dependent transmittance,<sup>8)</sup> the optimal cell retardation value,<sup>9)</sup> the cell gap-dependent driving voltage,<sup>10)</sup> and the external pressure-dependent dynamics<sup>11,12)</sup> depend on the sign of the LC.

In the LCDs, the transmittance of the LC cell depends on the cell retardation value, which is a multiplication of the cell gap ( $d$ ) and the birefringence ( $\Delta n$ ) of the LC. The LC cells, such as the IPS and TN<sup>13)</sup> cells, do show that the transmittance remains the same as long as the cell retardation value remains constant, regardless of whether either the cell gap, or the birefringence changes. However, the FFS mode that uses the LC with a negative dielectric anisotropy (-LC) does not follow the conventional rule, i.e., the transmittance decreases as the cell gap decreases, even though the cell retardation value remains the same.<sup>14)</sup> In this paper, we investigate the light transmittance of the FFS mode, as a function of the cell gap, when using the LC with a positive dielectric anisotropy (+LC). Then we find the origin of the transmittance decrease using simulations and experiments.

## 2. Switching Principle of the FFS Mode with the +LC and Simulation Conditions

In the FFS mode, the LCs are homogeneously aligned in

an initial state, in which the optic axis of the LC is coincident with one of the crossed polarizer axis. When using the -LC, the LC rotates almost in plane. Thus the normalized light transmission of a device is determined by the following equation

$$T/T_0 = \sin^2(2\psi(V)) \sin^2(\pi d \Delta n_{\text{eff}}(V)/\lambda) \quad (2.1)$$

where  $\psi$  is a voltage-dependent angle between the transmission axis of the crossed polarizers and the LC director,  $\Delta n_{\text{eff}}$  is a voltage-dependent effective birefringence and  $\lambda$  is the wavelength of the incident light. Before applying a bias voltage, the  $\psi$  is zero and thus the cell appears black. With respect to electrode structure, the FFS device only has electrodes on the bottom substrate. In general, a common electrode exists as a plane, and a pixel electrode exists above a passivation layer as a slit formed with a separation between pixel electrodes, in which both electrodes should be transparent, as shown in Fig. 1. With this electrode structure, a fringe-electric field having both horizontal ( $E_y$ ) and vertical ( $E_z$ ) field components is generated when voltage is applied. Consequently, the transmittance occurs with a bias voltage

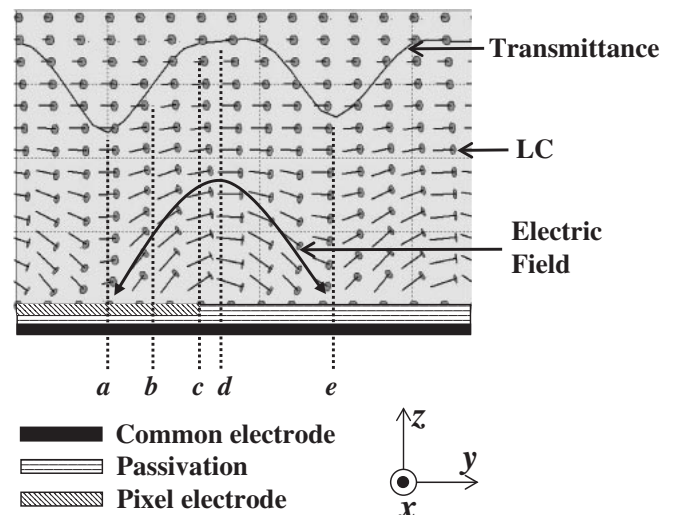


Fig. 1. Schematic cell structure and orientation of the LC molecules in the white state of the FFS mode using the +LC.

\*To whom correspondence should be addressed.  
 E-mail address: lsh1@chonbuk.ac.kr

for the  $-LC$  while the LC director experiences mainly twist deformation, however it occurs for the  $+LC$  while the LC director experiences twist deformation and a relatively large tilt angle, as appeared in Fig. 1. One significant detail is that the LC rotates the most around the middle of the cell at position  $a$  and  $e$ , however, at position  $c$  the LC near the electrode substrate twists most. This evidence enables one to consider the transmittance behavior intuitively and to reduce that both the IPS and the TN behavior are mixed with different weight percentages, since the transmittance in  $c$  is higher than that in  $a$ . Therefore, the transmittance in the FFS mode using a  $+LC$  in a white state can be described as

$$T/T_0 = A \sin^2(2\psi) \sin^2(B\pi d\Delta n/\lambda) + C \left( 1 - \frac{\sin^2(\pi/2\sqrt{1+(2Dd\Delta n/\lambda)^2})}{1+(2Dd\Delta n/\lambda)^2} \right) \quad (2.2)$$

where  $A$ ,  $B$ ,  $C$  and  $D$  are fitting parameters related to the transmittance and effective cell retardations.<sup>9)</sup> The first term and the second term in eq. (2.2) come from eq. (2.1), and Gooch and Terry's transmittance equation for the TN mode, respectively.

To understand the orientation of the  $+LC$  director in the voltage-on state, we first calculated the field distribution along the horizontal axis when  $z/d$  is 0.1, 0.5 and 0.9, where  $z$  indicates a vertical distance of the LC layer. Figure 2 shows the distribution of the field intensity of the horizontal

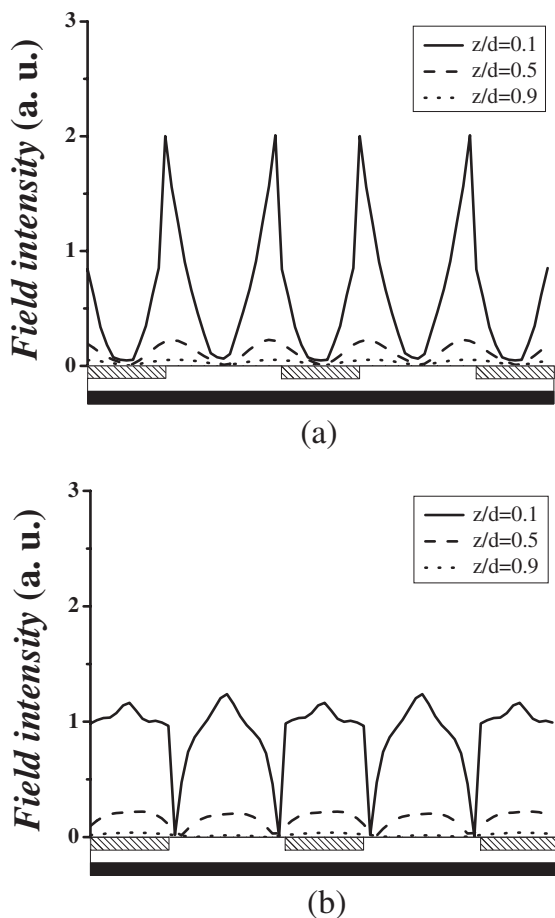


Fig. 2. Field distribution of the horizontal (a) and vertical (b) component in the FFS device along the horizontal plane at several vertical distances.

and vertical components, which exist along the horizontal direction in the FFS devices when a voltage of 4.4 V with respect to common electrode was applied to all pixel electrodes. As shown in Fig. 2, the field intensity of  $E_y$  near the edge of the pixel electrodes is maximal and rapidly drops to zero above the center of the electrodes. The field intensity also decreases rapidly as it moves away from the electrode surface. This implies that the deformation of the LC is much greater near the bottom surface than near the top surface. In the case of  $E_z$ , the maximum field intensity exists at the center of the electrodes, although it is relatively weaker than that of  $E_y$ . Similarly, it also decreases as it progresses away from the electrode surface. Such a field distribution, which is dependent on electrode position, causes the LCs to deform differently depending on whether the electrode position is subjected to tilt or twist angles. In particular, the  $+LC$  at a high tilt angle in position  $b$  is generated such that less twisting force is applied on the LC existing at position  $a$ , which results in a lower transmittance than that of the  $-LC$ . In addition, as the cell gap decreases, more LCs are affected by surface anchoring such that the LCs at position  $a$  are less twisted compared to LCs with a large cell gap. Thus, the transmittance decreases.

To obtain calculations, we used commercially available software, "LCD Master" (Shintech, Japan), where the motion of the LC director is calculated based on the Ericksen–Leslie theory and  $2 \times 2$  Jones matrix is applied to achieve the optical transmittance calculation. Here, the electrode and passivation thickness are 400 and 4500 Å, respectively. Comparatively, the pixel electrode width and the distance between them are 3 and 4.5 μm. The LC that has a positive dielectric anisotropy ( $\Delta\epsilon = 8.2$ ,  $K_1 = 9.7$  pN,  $K_2 = 5.2$  pN,  $K_3 = 13.3$  pN) is used. The initial rubbing direction is  $80^\circ$ , with respect to  $y$ -direction, and has a surface tilt angle of  $2^\circ$ . The strong anchoring at both substrates with anchoring energy much larger than  $10^{-6}$  J m $^{-2}$  is assumed such that the LCs do not rotate at the interface.

### 3. Calculated Results and Discussion

The transmittance is calculated as a function of the cell gap. To calculate this, the cell gap changes, while changing the  $\Delta n$  of the LC is varied, such that the cell retardation value (0.40 μm) remains the same. Normalized transmission at an operating voltage ( $V_{op}$ ) is decreased from 0.79 to 0.67 when the cell gap decreases from 4 to 2 μm, as shown in Fig. 3. To understand the origin of the decreased transmittance, the transmittance along the electrode position is calculated when it is maximal for three different cells, as shown in Fig. 4. As the dotted lines clearly indicate, the transmittance between the center and edge of the electrode decreases as the cell gap decreases, which is where the decreased transmittance of the cell with the 2 μm cell gap originates compared to the cell with 4 μm cell gap. Also, the transmittance at position  $d$  decreases slightly with the decreasing cell gap. To understand voltage-dependent transmittance along electrodes for the cells with different cell gaps in more detail, we investigated the electrode-position dependent transmittance when it was applied to voltages between,  $V_{op} - 0.5$  V ( $V_-$ ),  $V_{op}$  and  $V_{op} + 0.5$  V ( $V_+$ ), as shown in Fig. 5. When the cell gap is 4 μm, the transmittance (0.9) at position  $c$  is much higher than that (0.6) at

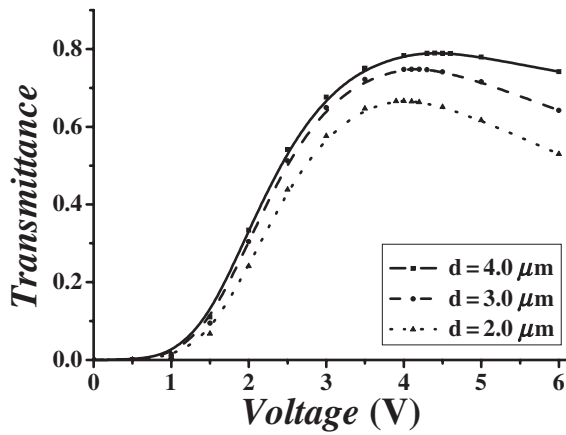


Fig. 3. Calculated voltage-dependent transmittance curves for the cells with different cell gaps.

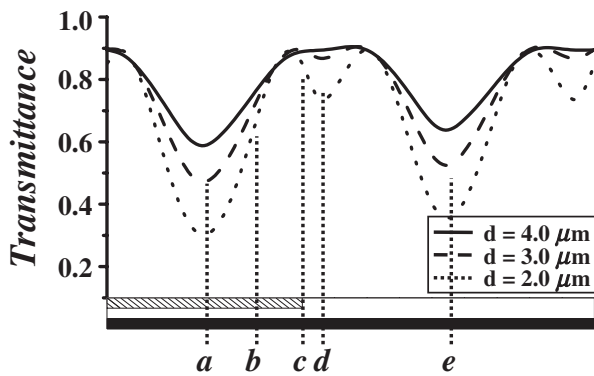


Fig. 4. Comparison of the transmittance distribution of the white state along the electrodes when the cell gap is 2, 3, and 4  $\mu\text{m}$ .

position *a* for an applied voltage of  $V_-$ . Further increasing voltage to  $V_+$ , the transmittance at positions *a* and *c* decreases, whereas it increases in an area between *a* and *c*. This results in a slightly decreased transmittance overall. This indicates that the transmittance difference of 0.3 between position *c* and *a* is an intrinsic problem, and that the LCs at positions *a* and *e* cannot be twisted further, even when a higher voltage is applied. When the cell gap is 3  $\mu\text{m}$ , the transmittance difference between positions *c* and *a* increases to 0.4. At  $V_-$ , and the transmittance is at a maximal level at position *c*. At  $V_{op}$ , it increases between positions *a* and *c*, but slightly decreases at position *d*. With further increasing voltage to  $V_+$ , it remains about the same between positions *a* and *c* but decreases at position *d*. When the cell gap is 2  $\mu\text{m}$ , the transmittance at *a* and *c* is much lower than that of cells having 3  $\mu\text{m}$ , or 4  $\mu\text{m}$  cell gaps, at all three different voltages and the transmittance difference between positions *c* and *a* increases to 0.55. By increasing the voltage from  $V_-$  to  $V_+$ , the transmittance at position *d* decreases while it remains about the same at position *a*. To summarize, as the cell gap decreases from 4 to 2  $\mu\text{m}$ , the transmittance decreases from 0.59 to 0.3 at position *a*, and from 0.89 to 0.85 at position *c*.

To understand in detail, the electrode-position dependent transmittance as a function of applied voltage and decreased transmittance at a low cell gap, we have calculated the

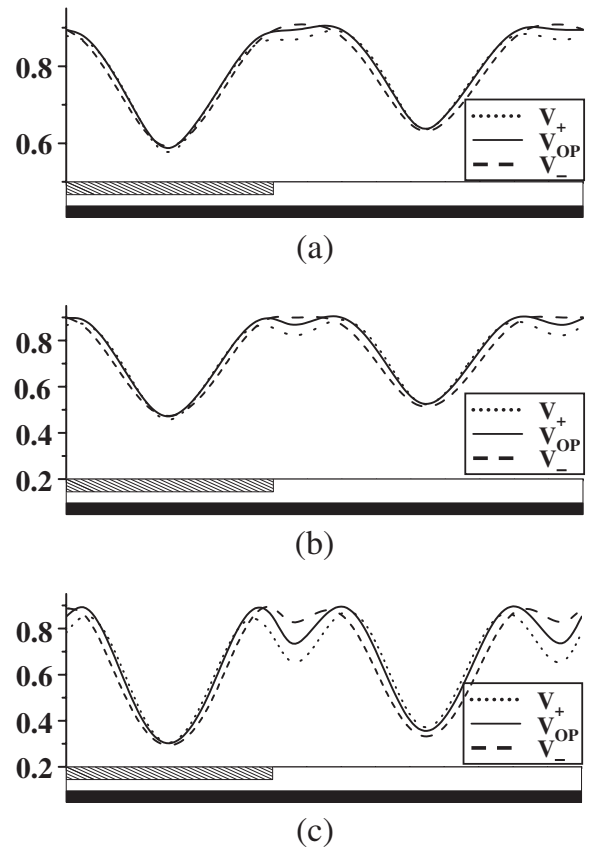


Fig. 5. Transmittance distribution along electrodes at three different voltages when the cell gap is (a) 4  $\mu\text{m}$ , (b) 3  $\mu\text{m}$  and (c) 2  $\mu\text{m}$ .

orientation of LCs for the +LC along the cell gap. Since the transmittance between *a* and *e* is a repeated basic unit we calculated the director profile at only four positions: *a*, *b*, *c* and *d*. Figure 6 shows the twist angle as a function of applied voltage, for these four different positions, when the cell gap is 2 and 4  $\mu\text{m}$ , respectively. In comparison to the twist angle in the white state at position *a*, the twisted angles from the original orientation are 21 and 32° at  $z/d = 0.4$  for the 2 and the 4  $\mu\text{m}$  cells, respectively. From this position, the transmittance follows the first term of eq. (2.2) such that a higher twist angle generates a higher transmittance, only if the tilt angles are approximately equal. At position *b*, the maximal twisted angles from the original position are 36° at  $z/d = 0.35$  and 44° at  $z/d = 0.225$  for the 2  $\mu\text{m}$  and the 4  $\mu\text{m}$  cells, respectively. The data indicates that, as the cell gap decreases more LCs are affected by surface anchoring, such that maximal twist deformation occurs at a higher vertical position for the 2  $\mu\text{m}$  cell than the 4  $\mu\text{m}$  cell. At positions *c* and *d*, the strong twist deformation occurs for both cells due to strong horizontal field intensity near the bottom substrate. For the 4  $\mu\text{m}$  cell at position *d*, the maximum twist angle occurs at  $z/d = 0.125$  and decreases linearly as it approaches the top substrate. It also reaches to 9° at 4.4 V ( $V_{op}$ ), i.e., the maximal twist angle at that vertical position is 71°. According to eq. (2.1), the transmittance at this voltage should be much lower than 0.92 because the  $\psi$  value exceeds 45°, however, at this position the transmittance reaches 0.92. This indicates that the optical calculation at this position is similar to that of the low twisted TN. For the 2  $\mu\text{m}$  cell at position *d*, the maximum

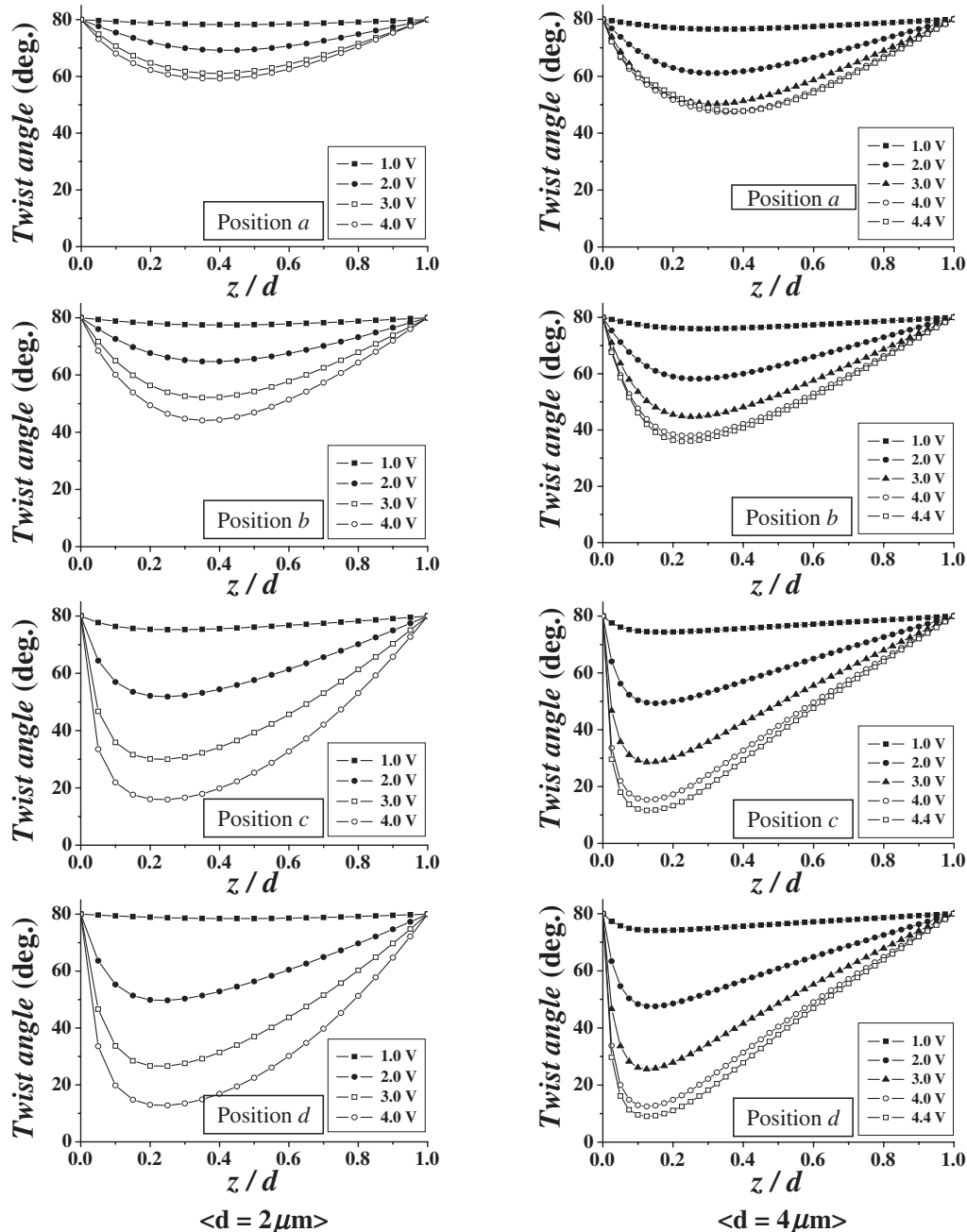


Fig. 6. Distribution of the LC's twist angle as a function of the applied voltage at four different positions *a*, *b*, *c* and *d* when the cell gap is 2 and 4  $\mu\text{m}$ .

twist angle occurs at  $z/d = 0.25$  and the maximal value is reached at  $13^\circ$  at 4.0 V ( $V_{\text{op}}$ ), i.e., the maximal twist angle at that vertical position is  $67^\circ$ . In contrast to the 4  $\mu\text{m}$  cell, the twist angle does not decrease linearly as it approaches the top substrate at every voltage larger than the Fredericks transition voltage. In addition, the twist angle at 3.0 V at  $z/d = 0.5$  is  $43^\circ$  and  $31^\circ$  for the 2  $\mu\text{m}$  and the 4  $\mu\text{m}$  cells, respectively. This indicates that the average twist angle is much larger in the 2  $\mu\text{m}$  cell than that in the 4  $\mu\text{m}$  cell. A large twist angle with such a distribution decreases the transmittance to 0.74 at  $V_{\text{op}}$ . Since the effective cell retardation at normal direction is not only determined by twist angle, but also by tilt angle, the tilt angle distribution is also calculated for the 2  $\mu\text{m}$  and the 4  $\mu\text{m}$  cells, as indicated in Fig. 7. At position *a*, the small tilt angle of less than  $10^\circ$

occurs near the bottom surface for both cells. Thus, at this position the transmittance is mainly determined by the twist angle. However, relatively large tilt angles below  $z/d = 0.3$  for both cells are generated at positions *b* and *c*. Thus, the average tilt angles are 17 and  $13^\circ$  at positions *b* and *c* for the 2  $\mu\text{m}$  cell while they are 14 and  $9^\circ$  at positions *b* and *c* for the 4  $\mu\text{m}$  cell. From the tilt angle distribution, we can calculate that the larger tilt angle at positions *b* and *c* in the 2  $\mu\text{m}$  cell causes a smaller twist angle and decreased transmittance at position *a* when compared to those in the 4  $\mu\text{m}$  cell. Furthermore, since the low transmittance at position *a* is the result of a competition between the elastic torque needed to twist the LC, and the elastic force needed to hold the LC at its initial state, we can deduce from surface anchoring that lowering the cell gap decreases transmittance. Nevertheless,

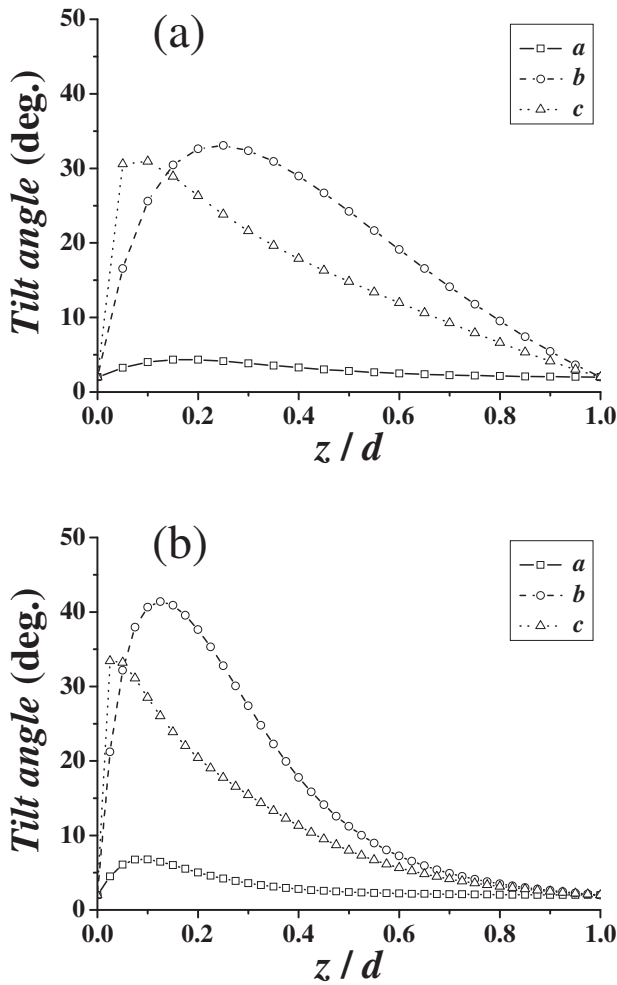


Fig. 7. Distribution of the LC's tilt angle at three different positions *a*, *b* and *c* when the cell gap is (a) 2 μm and (b) 4 μm.

some suggestions that increase the elastic or dielectric torque can be made such that decreasing electrode width and distance increases a horizontal field density, resulting in improved transmittance of the FFS cell using the +LC.<sup>15)</sup>

#### 4. Experimental Results and Discussion

To confirm the calculated results, test cells were fabricated. The electrode width and the distance between electrodes was 3 and 5.5 μm, respectively. Two LC cells with a cell gap of 2.4 and 3.8 μm were also made. LC1 ( $\Delta n = 0.166$  at  $\lambda = 589$  nm,  $\Delta \epsilon = 9.3$ ) and LC2 ( $\Delta n = 0.099$  at  $\lambda = 589$  nm,  $\Delta \epsilon = 8.2$ ) were placed in the cells with 2.4 and 3.8 μm cell gap, respectively. The cell retardation values for two cells were 0.398 and 0.376 μm, respectively.

For the electro-optic measurements, the sample cell was subjected to the following controls: a Halogen lamp was used as a light source, and a square wave of 60 Hz voltage was applied by a function generator. Light passing through the cell was detected by a photomultiplier tube at room temperature. Figure 8 shows the voltage-dependent transmittance curves for the two different cells. The cell with a 2.4 μm cell gap shows a lower transmittance than the cell with the 3.8 μm cell gap, although the first has an optimal cell retardation value that reaches a maximal transmittance.<sup>9)</sup> This corresponds to the calculated results. To understand

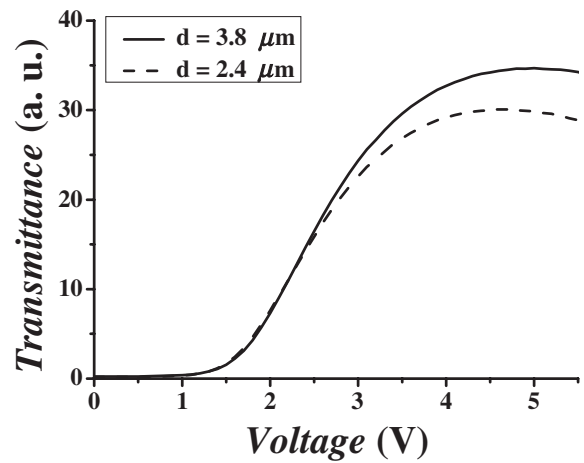


Fig. 8. Measured voltage-dependent transmittance curves for the cells with different cell gaps.

how the LC director responds to an applied voltage along the electrode, the voltage-dependent LC texture was observed using optical polarizing microscopy. Here, the light source intensity was adjusted to show a good contrast along the electrodes. Figure 9 shows microphotographs of the cell, together with the calculated transmittance profile. For the cell with a 2.4 μm cell gap, the mid-grey transmittance is the highest (about 0.61) at position *d*, and the lowest (about 0.18) at position *e* according to the calculated results, which correspond to the experimental results. Increasing the voltage to the white-state, the calculated transmittance at position *c* increases to about 0.88 while the transmittance at positions *a* and *e* increases to about 0.39 and 0.45, respectively. Again, the observed results agree with calculated results. For the cell with the 3.8 μm cell gap, transmittance at mid-grey is highest (about 0.55) at position *d* and lowest (about 0.29) at position *e*. Compared to the 2 μm cell, the intensity difference between positions *a* and *c* is significantly reduced in the 4 μm cell. When the 3.8 μm cell is at the white state, the calculated transmittance at position *a* and *d* reaches 0.59 and 0.89, respectively. Both these values are higher than those in the 2 μm cell. The observed transmittance also shows that the intensity difference between the two positions is reduced. These results can be summarized as follows: First, the experimental results clearly prove that the total transmittance of the FFS cell with a large cell gap is higher than with a small cell gap. This is true when using the LC with a positive dielectric anisotropy, and similar to that when using the -LC, though the decreasing ratio differs from one another. Second, the low transmittance at position *a* compared to position *d* for both cells is caused by the fact that the LCs are not fully twisted, due to weak elastic torque on the LCs at position *a*, the result of a high tilt at position *b*. Third, as the cell gap decreases, the elastic torque needed to twist the LCs at position *a* is overcome by the increased elastic force that holds the LCs in an original state.

#### 5. Conclusion

Voltage-dependent transmittance and LC deformation, as a function of the cell gap, have been studied in the FFS mode when the LC with a positive dielectric anisotropy is used. In

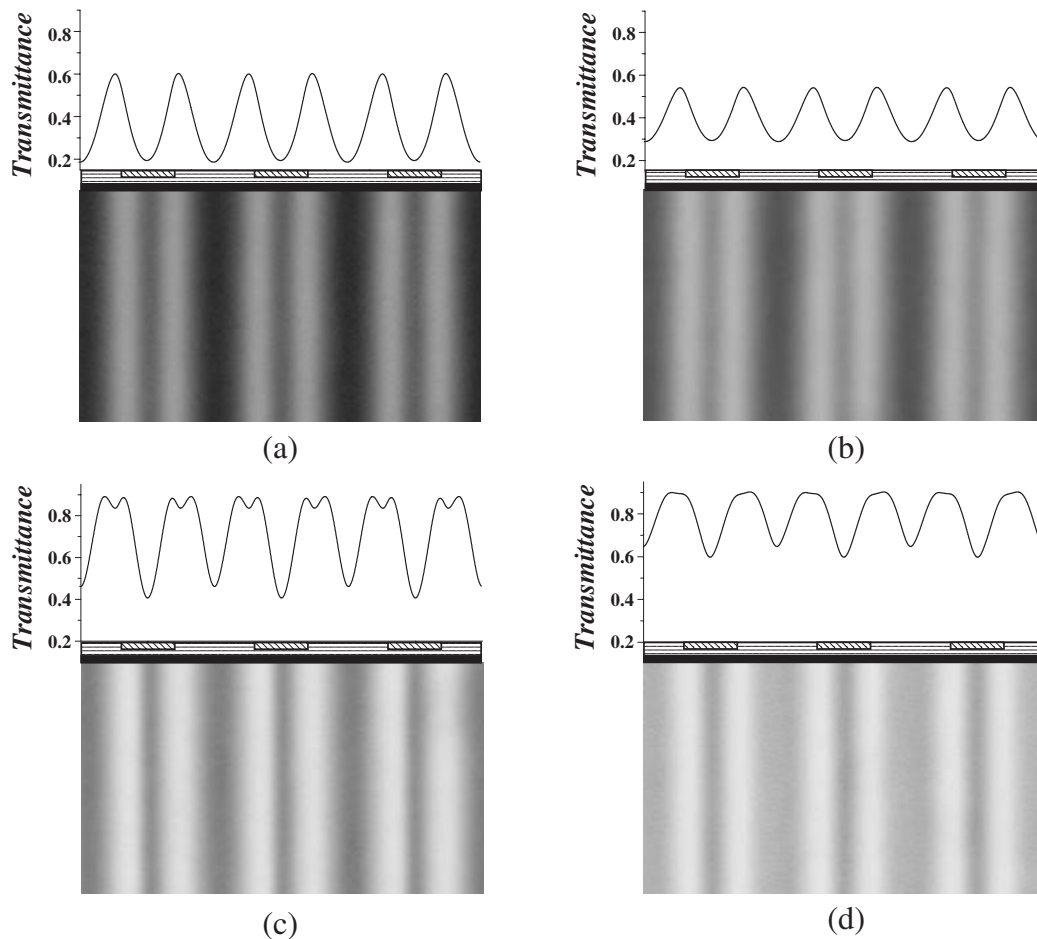


Fig. 9. Microphotograph of the FFS cells showing how the intensity of transmittance is changing along the electrodes at the mid-grey area with cell gaps of (a)  $2.4\ \mu\text{m}$  and (b)  $3.8\ \mu\text{m}$  and at the white state with cell gaps of (c)  $2.4\ \mu\text{m}$  and (d)  $3.8\ \mu\text{m}$ .

this device, when cell gap decreases from  $4$  to  $2\ \mu\text{m}$ , the transmittance of the  $2\ \mu\text{m}$  cell is strongly dependent on the electrode position, which results in a lower transmittance than in the  $4\ \mu\text{m}$  cell. The transmittance at the center of the pixel and common electrode is especially low because the LC's tilt angle between the edge and center of electrodes increases as the cell gap decreases, such that the twist elastic force necessary to rotate the LC at the center of electrodes is reduced. Further, as the cell gap decreases more LCs are affected by surface anchoring. This means that the LCs at the center of electrodes that do not have a horizontal field intensity experience more difficulty rotating as the cell gap decreases.

#### Acknowledgements

This research was supported by the Program for the Training of Graduate Students in Regional Innovation, which was conducted by the Ministry of Commerce, Industry and Energy of the Korean Government.

1) B. Kiefer, B. Weber, F. Windscheid and G. Baur: Proc. 12th Int. Display Research Conf., Society for Information Display and the Institute of Television Engineers of Japan, Hiroshima, 1992, p. 547.

- 2) M. Oh-e and K. Kondo: Appl. Phys. Lett. **67** (1995) 3895.
- 3) K. Kondo, S. Matsuyama, N. Konishi and H. Kawakami: SID 98 Dig., 1998, p. 389.
- 4) S. H. Lee, S. L. Lee and H. Y. Kim: Proc. 18th Int. Display Research Conf., Society for Information Display and the Institute of Television Engineers of Japan, Hiroshima, 1998, p. 371.
- 5) S. H. Lee, S. L. Lee and H. Y. Kim: Appl. Phys. Lett. **73** (1998) 2881.
- 6) S. H. Lee, S. L. Lee, H. Y. Kim and T. Y. Eom: J. Korean Phys. Soc. **35** (1999) S1111.
- 7) S. H. Lee, S. M. Lee, H. Y. Kim, J. M. Kim, S. H. Hong, Y. H. Jeong, C. H. Park, Y. J. Choi, J. Y. Lee, J. W. Koh and H. S. Park: SID '01 Dig., 2001, p. 484.
- 8) S. H. Hong, I. C. Park, H. Y. Kim and S. H. Lee: Jpn. J. Appl. Phys. **39** (2000) L527.
- 9) S. H. Jung, H. Y. Kim, S. H. Song, J. H. Kim, S. H. Nam and S. H. Lee: Jpn. J. Appl. Phys. **43** (2004) 1028.
- 10) H. Y. Kim, S. H. Hong, J. M. Rhee and S. H. Lee: Liq. Cryst. **30** (2003) 1287.
- 11) J.-D. Noh, H. Y. Kim, J. M. Kim, J. W. Koh, J. Y. Lee, H. S. Park and S. H. Lee: SID '02 Dig., 2002, p. 224.
- 12) H. Y. Kim, S. H. Nam and S. H. Lee: Jpn. J. Appl. Phys. **42** (2003) 2752.
- 13) C. H. Gooch and H. A. Tarry: J. Phys. D **8** (1975) 1575.
- 14) S. H. Jung, H. Y. Kim, M.-H. Lee, J. M. Rhee and S. H. Lee: Liq. Cryst. **32** (2005) 267.
- 15) Y. M. Jeon, I. S. Song, S. H. Lee, H. Y. Kim, S. Y. Kim and Y. J. Lim: SID '05 Dig., 2005, p. 328.